

Superconductivity in the two-dimensional t - t' -Hubbard model

Andreas Eberlein¹ and Walter Metzner¹

¹Max Planck Institute for Solid State Research, D-70569 Stuttgart, Germany

(Dated: September 24, 2018)

Using a recently developed renormalization group method for fermionic superfluids, we determine conditions for d -wave superconductivity in the ground state of the two-dimensional Hubbard model at moderate interaction strength, and we compute the pairing gap in the superconducting regime. A pairing instability signaled by a divergent flow in the Cooper channel leads to a superconducting state in all studied cases. The next-to-nearest neighbor hopping t' plays a crucial role in the competition between antiferromagnetism and superconductivity. A sizable t' is necessary to obtain a sizable pairing gap.

PACS numbers: 71.10.Fd, 74.20.-z, 75.10.-b

I. INTRODUCTION

Shortly after the discovery of high-temperature superconductivity in layered cuprate compounds, Anderson¹ suggested that the two-dimensional Hubbard model contains the essence of the electron dynamics in the copper-oxygen planes. While it may not describe all relevant aspects of the system, the Hubbard model definitely captures its most prominent property, that is, d -wave superconductivity in the vicinity of antiferromagnetic order.² Convincing evidence for superconductivity in the Hubbard model at weak and moderate coupling strengths has been established by self-consistent or renormalized perturbation expansions,³⁻⁶ and from functional renormalization group flows.⁷⁻⁹ At stronger coupling, embedded cluster methods¹⁰ yield superconducting states in a large density range, if magnetic order is excluded,¹¹⁻¹³ and otherwise surprisingly extended regions of superconductivity with a sizable pairing gap coexisting with antiferromagnetism.¹⁴⁻¹⁶ Variational Monte Carlo calculations with superconducting trial wave functions revealed a substantial energy gain from d -wave pairing in a wide density range in the strong coupling regime.¹⁷ On the other hand, unbiased quantum Monte Carlo (QMC) simulations frequently detected enhanced superconducting fluctuations, but only rarely evidence for long-range order.¹⁸

At weak and moderate coupling the functional renormalization group (fRG) is probably the most powerful method for studying the interplay of magnetism and superconductivity in two-dimensional lattice electron models.¹⁹ In this method, approximations are derived by truncating an exact flow equation for the effective action, where the flow parameter Λ is usually an energy scale controlling the successive integration of fluctuations.²⁰ The fRG treats all fluctuation contributions to the effective two-particle interaction and self-energy on equal footing and in the thermodynamic limit. The d -wave pairing instability generated by magnetic fluctuations in the two-dimensional Hubbard model emerges already within the lowest order (one-loop) truncation.⁷⁻⁹ The instability is signaled by a divergence of the effective two-

particle interaction in the Cooper channel at a critical cutoff scale Λ_c .

Antiferromagnetic fluctuations are the main mechanism for d -wave pairing interactions, at least for a moderate Hubbard interaction, but magnetism also competes with superconductivity, since magnetic order (static or fluctuating) leads to gaps in the electronic spectrum. From the early fRG flows⁷⁻⁹ the competition between antiferromagnetism and superconductivity could not be decided unambiguously in a sizable density range where both channels develop large effective interactions, since the flow had to be stopped at the scale at which the effective interaction diverges, and it was not clear whether the leading divergence is a reliable indicator for the prevailing type of order.

To continue the flow beyond the critical scale one has to allow for spontaneous symmetry breaking. One possibility is to introduce a bosonic order parameter field by a Hubbard-Stratonovich decoupling of the interaction. This approach to symmetry breaking in the fRG has already been applied to antiferromagnetic²¹ and superconducting^{22,23} states in the Hubbard model. The choice of a specific decoupling procedure of the Hubbard interaction introduces a certain bias, which leads to ambiguities in cases with competing instabilities. Alternatively, one may work with a purely fermionic flow, which is the route we take here. In the fermionic fRG, a relatively simple one-loop truncation with self-energy feedback²⁴ solves mean-field models of symmetry breaking such as the reduced BCS model exactly, although the effective interaction diverges at Λ_c .²⁵ For the *attractive* Hubbard model, this truncation yields results for the pairing gap in good agreement with earlier estimates at weak and moderate coupling strength.²⁶ Recently, an improved parametrization of the interaction vertex in a fermionic superfluid, which fully exploits spin rotation invariance and parametrizes singularities by a single momentum and frequency variable, was derived.^{27,28} It is based on an extension of a decomposition of the normal-state vertex in charge, magnetic, and pairing channels^{29,30} to the superfluid state. This new parametrization was also applied to the attractive Hubbard model, and a comprehensive understanding

of the behavior of the flowing effective interaction was obtained.²⁸

In the present work, we use the fermionic fRG to detect and analyze superconductivity in the ground state of the two-dimensional *repulsive* Hubbard model. We find that a diverging d -wave pairing interaction always leads to a superconducting state, and we compute the d -wave gap as a function of doping for various choices of the next-to-nearest neighbor hopping t' . The results reveal the crucial role of t' in the competition between magnetism and superconductivity.

The paper is structured as follows. In Sec. II we describe the fRG equations for an unbiased detection and analysis of d -wave superconducting states in the two-dimensional Hubbard model. In Sec. III we present results for effective interactions, critical scales and the ground state pairing gap. A short summary and final remarks in Sec. IV close the presentation.

II. MODEL AND METHOD

In standard second-quantization notation the Hubbard model³¹ is described by the Hamiltonian

$$H = \sum_{\mathbf{j}, \mathbf{j}', \sigma} t_{\mathbf{j}\mathbf{j}'} c_{\mathbf{j}\sigma}^\dagger c_{\mathbf{j}'\sigma} + U \sum_{\mathbf{j}} n_{\mathbf{j}\uparrow} n_{\mathbf{j}\downarrow}, \quad (1)$$

where \mathbf{j}, \mathbf{j}' label lattice sites and σ is the spin orientation. For nearest and next-to-nearest neighbor hopping on a square lattice with amplitudes $-t$ and $-t'$, respectively, the Fourier transform of the hopping matrix yields a dispersion $\epsilon_{\mathbf{k}} = -2t(\cos k_x + \cos k_y) - 4t' \cos k_x \cos k_y$. We set $t = 1$, which defines our unit of energy.

The partition function and generating functionals for correlation functions can be written as functional integrals over anticommuting fields $\psi_{k\sigma}$ and $\bar{\psi}_{k\sigma}$, where $k = (k_0, \mathbf{k})$ comprises Matsubara frequencies and momenta. The generating functional Γ for one-particle irreducible vertex functions, also known as *effective action*, is given by the Legendre transform of the generating functional for connected Green functions.³² Adding a suitable regulator term to the quadratic part of the bare action, one can define a scale dependent effective action Γ^Λ that interpolates smoothly between the bare action \mathcal{S} at the highest scale Λ_0 and the final effective action Γ for $\Lambda \rightarrow 0$. The flow of Γ^Λ obeys an exact functional flow equation,³³ from which one can derive a hierarchy of flow equations for the vertex functions.

To describe a superfluid state, it is convenient to use a representation in terms of *Nambu* fields $\phi_{k_s}, \bar{\phi}_{k_s}$ defined as $\phi_{k_+} = \psi_{k\uparrow}, \bar{\phi}_{k_+} = \bar{\psi}_{k\uparrow}, \phi_{k_-} = \bar{\psi}_{-k\downarrow}, \bar{\phi}_{k_-} = \psi_{-k\downarrow}$. To quartic order in the fields, the scale dependent effective

action for a spin-singlet superfluid has the general form³⁴

$$\begin{aligned} \Gamma^\Lambda[\phi, \bar{\phi}] &= \Gamma^{(0)\Lambda} - \sum_k \sum_{s_1, s_2} \Gamma_{s_1 s_2}^{(2)\Lambda}(k) \bar{\phi}_{k s_1} \phi_{k s_2} \\ &+ \frac{1}{4} \sum_{k_1, \dots, k_4} \sum_{s_1, \dots, s_4} \Gamma_{s_1 s_2 s_3 s_4}^{(4)\Lambda}(k_1, k_2, k_3, k_4) \\ &\times \bar{\phi}_{k_1 s_1} \bar{\phi}_{k_2 s_2} \phi_{k_3 s_3} \phi_{k_4 s_4}. \end{aligned} \quad (2)$$

For systems with (unbroken) spin-rotation invariance, only terms with an equal number of ϕ and $\bar{\phi}$ fields contribute. The Nambu vertex $\Gamma_{s_1 s_2 s_3 s_4}^{(4)\Lambda}(k_1, k_2, k_3, k_4)$ is nonzero only for $k_1 + k_2 = k_3 + k_4$. The Nambu components of the 2-point function $\Gamma_{s_1 s_2}^{(2)\Lambda}(k)$ form a 2×2 matrix $\mathbf{\Gamma}^{(2)\Lambda}(k)$. Its matrix inverse is the Nambu propagator

$$\mathbf{G}^\Lambda(k) = \begin{pmatrix} G^\Lambda(k) & F^\Lambda(k) \\ F^{*\Lambda}(k) & -G^\Lambda(-k) \end{pmatrix}, \quad (3)$$

where $G^\Lambda(k) = -\langle \psi_{k\sigma} \bar{\psi}_{k\sigma} \rangle$ and $F^\Lambda(k) = -\langle \psi_{k\uparrow} \psi_{-k\downarrow} \rangle$. The Dyson equation $(\mathbf{G}^\Lambda)^{-1} = (\mathbf{G}_0^\Lambda)^{-1} - \Sigma^\Lambda$ relates the full propagator \mathbf{G}^Λ to the self-energy Σ^Λ and the bare regularized propagator \mathbf{G}_0^Λ given by

$$[\mathbf{G}_0^\Lambda(k)]^{-1} = \begin{pmatrix} ik_0 - \xi_{\mathbf{k}} + R^\Lambda(k_0) & \Delta_0(k) \\ \Delta_0^*(k) & ik_0 + \xi_{\mathbf{k}} + R^\Lambda(k_0) \end{pmatrix}, \quad (4)$$

where $\xi_{\mathbf{k}} = \epsilon_{\mathbf{k}} - \mu$, and $\Delta_0(k)$ is a small initial gap added to the bare action to trigger the symmetry breaking. It can be chosen small enough to avoid a discernible effect on the gap at the end of the flow. The regulator function $R^\Lambda(k_0) = i \operatorname{sgn}(k_0) \sqrt{k_0^2 + \Lambda^2} - ik_0$ replaces frequencies k_0 with $|k_0| \ll \Lambda$ by $\operatorname{sgn}(k_0)\Lambda$ and thus confines the bare propagator to a size of order Λ^{-1} . The self-energy matrix has the form

$$\Sigma^\Lambda(k) = \begin{pmatrix} \Sigma^\Lambda(k) & \Delta_0(k) - \Delta^\Lambda(k) \\ \Delta_0^*(k) - \Delta^{\Lambda*}(k) & -\Sigma^\Lambda(-k) \end{pmatrix}, \quad (5)$$

where $\Delta^\Lambda(k)$ is the flowing gap function.

The Nambu self-energy obeys the exact flow equation

$$\frac{d}{d\Lambda} \Sigma_{s_1 s_2}^\Lambda(k) = \sum_{k'} \sum_{s'_1, s'_2} S_{s_2 s'_1}^\Lambda(k') \Gamma_{s_1 s'_1 s'_2 s_2}^{(4)\Lambda}(k, k', k', k), \quad (6)$$

where $\mathbf{S}^\Lambda(k) = \frac{d}{d\Lambda} \mathbf{G}^\Lambda(k) \Big|_{\Sigma^\Lambda \text{ fixed}}$. The flow of the Nambu vertex $\Gamma^{(4)\Lambda}$ is approximated by a one-loop truncation with self-energy feedback²⁴ where contributions from three-particle interactions leading to two- and higher loop terms are neglected. This approximation is exact for mean-field models such as the reduced BCS model.²⁵ The flow equation for $\Gamma^{(4)\Lambda}$ is then given by a sum of three one-loop diagrams corresponding to the particle-particle, direct and crossed particle-hole channel, respectively.^{27,28}

The parametrization of the Nambu vertex is based on an extension of the channel decomposition devised initially for the normal state^{29,30} to a spin-singlet superfluid. The fluctuation contributions to the normal effective interaction are decomposed in a charge, a magnetic, and a

pairing contribution, where possible singular momentum and frequency dependences of the corresponding coupling functions $C_{\mathbf{k}\mathbf{k}'}^\Lambda(q)$, $M_{\mathbf{k}\mathbf{k}'}^\Lambda(q)$, and $P_{\mathbf{k}\mathbf{k}'}^\Lambda(q)$ are isolated in the variable q , which is either a momentum transfer or a conserved total momentum (or frequency). In a superfluid state also anomalous interactions appear. A coupling function $W_{\mathbf{k}\mathbf{k}'}^\Lambda(q)$ describes the destruction or creation of four electrons, while another function $X_{\mathbf{k}\mathbf{k}'}^\Lambda(q)$ captures anomalous processes with three ingoing electrons and one outgoing electron, or vice versa.^{27,28}

We adopt a static approximation for the vertex, that is, we discard the frequency dependences of the coupling functions. The q_0 -frequency dependence of the coupling functions is crucial for capturing the dynamics of infrared singularities associated with the Goldstone boson,²⁸ but this has little impact on the gap function. By fixing the phase of the gap at zero, the gap function and all (static) coupling functions are real. In the normal and anomalous pairing channels it is convenient to use amplitude and phase coupling functions defined as $A_{\mathbf{k}\mathbf{k}'}^\Lambda(\mathbf{q}) = P_{\mathbf{k}\mathbf{k}'}^\Lambda(\mathbf{q}) + W_{\mathbf{k}\mathbf{k}'}^\Lambda(\mathbf{q})$ and $\Phi_{\mathbf{k}\mathbf{k}'}^\Lambda(\mathbf{q}) = P_{\mathbf{k}\mathbf{k}'}^\Lambda(\mathbf{q}) - W_{\mathbf{k}\mathbf{k}'}^\Lambda(\mathbf{q})$, respectively. The dependence of the coupling functions on the fermionic momenta \mathbf{k} and \mathbf{k}' is parametrized by an expansion in the simplest s -wave and d -wave form factors, $s_{\mathbf{k}} = 1$ and $d_{\mathbf{k}} = \cos k_x - \cos k_y$, respectively:

$$\begin{aligned} C_{\mathbf{k}\mathbf{k}'}^\Lambda(\mathbf{q}) &= C_s^\Lambda(\mathbf{q}) + C_d^\Lambda(\mathbf{q})d_{\mathbf{k}}d_{\mathbf{k}'}, \\ M_{\mathbf{k}\mathbf{k}'}^\Lambda(\mathbf{q}) &= M_s^\Lambda(\mathbf{q}) + M_d^\Lambda(\mathbf{q})d_{\mathbf{k}}d_{\mathbf{k}'}, \\ A_{\mathbf{k}\mathbf{k}'}^\Lambda(\mathbf{q}) &= A_s^\Lambda(\mathbf{q}) + A_d^\Lambda(\mathbf{q})d_{\mathbf{k}}d_{\mathbf{k}'}, \\ \Phi_{\mathbf{k}\mathbf{k}'}^\Lambda(\mathbf{q}) &= \Phi_s^\Lambda(\mathbf{q}) + \Phi_d^\Lambda(\mathbf{q})d_{\mathbf{k}}d_{\mathbf{k}'}, \\ X_{\mathbf{k}\mathbf{k}'}^\Lambda(\mathbf{q}) &= X_{sd}^\Lambda(\mathbf{q})d_{\mathbf{k}'} + X_{ds}^\Lambda(\mathbf{q})d_{\mathbf{k}}. \end{aligned} \quad (7)$$

For the first four coupling functions, mixed s - d -terms are very small and can be neglected.³⁵ On the other hand, the last one is dominated by mixed terms, while diagonal s - s - and d - d -terms are negligible here. The neglected terms are fully absent in a mean-field model with reduced s - and d -wave interactions in the forward scattering and pairing channels.³⁶ The \mathbf{q} -dependences of the coupling functions cannot be parametrized accurately by simple functions and are therefore discretized on a two-dimensional grid.

Inserted into the flow equation (6), a static real vertex entails a frequency-independent real self-energy. The momentum dependence of its normal component is weak and has no important effects.³⁷ We therefore approximate Σ^Λ by a constant. For the momentum dependence of the gap function we use the simplest d -wave ansatz $\Delta^\Lambda(\mathbf{k}) = \Delta^\Lambda d_{\mathbf{k}}$, and correspondingly $\Delta_0(\mathbf{k}) = \Delta_0 d_{\mathbf{k}}$.

The flow of the coupling functions, self-energy and gap is obtained by projecting the right hand sides of the flow equations on the ansatz via Fermi surface averages.²⁸ Deviations from the Ward identity relating gap and vertex are eliminated during the flow by another projection.^{28,36}

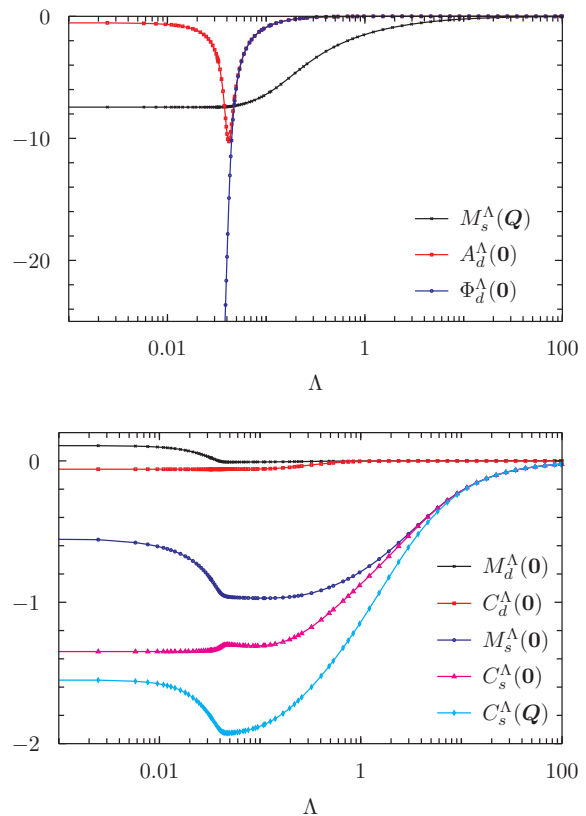


FIG. 1: (Color online) Flows of coupling functions for $U = 3$, $t' = -0.25$, and density $n = 0.9$. Top: Dominant magnetic and d -wave pairing coupling functions at $\mathbf{q} = \mathbf{Q} = (\pi, \pi)$ and $\mathbf{q} = \mathbf{0}$, respectively. Bottom: Charge coupling functions at $\mathbf{q} = \mathbf{0}$ and $\mathbf{q} = (\pi, \pi)$, and magnetic coupling functions at $\mathbf{q} = \mathbf{0}$. Note the distinct scales on the vertical axes of the top and bottom panel.

III. RESULTS

We now present results based on a numerical solution of the flow equations. In Fig. 1 we show the flow of various coupling functions at fixed momenta for a moderate interaction strength $U = 3$, a next-to-nearest neighbor hopping $t' = -0.25$, and density $n = 0.9$. For these parameters the ground state is a d -wave superconductor with a gap amplitude $\Delta(0, \pi) = 2\Delta^{\Lambda=0} = 0.047$. The pairing instability at $\Lambda_c = 0.040$ is generated mostly by antiferromagnetic fluctuations. The latter grow gradually already at scales well above Λ_c , as can be seen from the flow of $M_s^\Lambda(\mathbf{q})$ at $\mathbf{q} = (\pi, \pi)$. The d -wave pairing amplitude coupling $A_d^\Lambda(\mathbf{0})$ exhibits a pronounced peak at the critical scale Λ_c . The presence of a small external pairing gap ($\Delta_0 = 1.6 \times 10^{-4}$) prevents a divergence of the peak. The phase coupling $\Phi_d^\Lambda(\mathbf{0})$ increases rapidly at Λ_c and saturates at a large final value proportional to Δ_0^{-1} .

Other coupling functions remain relatively small. Some examples are shown in the lower panel of Fig. 1. In

particular, the d -wave charge coupling function $C_d^\Lambda(\mathbf{q})$ is only weakly attractive for all wave vectors \mathbf{q} . A large negative $C_d^\Lambda(\mathbf{0})$ would indicate an incipient d -wave Pomeranchuk instability^{8,38} toward nematic order.³⁹ A strongly attractive $C_d^\Lambda(\mathbf{q})$ at $\mathbf{q} \neq \mathbf{0}$ would signal a modulated nematic instability,⁴⁰ which can also be viewed as a d -wave bond order. Such an instability was shown to accompany d -wave pairing near an antiferromagnetic quantum critical point.⁴¹ However, a recent fRG study of the Hubbard model above the critical scale Λ_c did not reveal any proximity to d -wave charge order,⁴² in agreement with our results.

The leading instabilities are generically either antiferromagnetism or d -wave pairing. In the upper panel of Fig. 2 we show the critical scale Λ_c as a function of “doping” $x = 1 - n$ at a fixed interaction strength $U = 3$ for various choices of t' . The doping range covers a broad regime from moderate electron doping to fairly large hole doping. Distinct symbols for d -wave superconductivity, commensurate and incommensurate antiferromagnetism indicate which coupling function diverges at Λ_c . Incommensurate antiferromagnetism is signaled by a divergence of $M_s(\mathbf{q})$ at wave vectors of the form $(\pi \pm \delta, \pi)$ and $(\pi, \pi \pm \delta)$. Note that Λ_c is maximal *above* Van Hove filling for all $t' < 0$. This is due to a mutual reinforcement of different channels in the presence of antiferromagnetic hot spots.⁴³

Whenever pairing is the leading instability, we continue the flow to $\Lambda = 0$ and compute the d -wave pairing gap. In the lower panel of Fig. 2 the resulting gap amplitudes $\Delta(0, \pi) = 2\Delta^{\Lambda=0}$ are plotted as a function of doping. One can see that $\Delta(0, \pi)$ is comparable to Λ_c .⁴⁴ Fluctuations below Λ_c have little influence on the size of the gap. An important observation is that in all cases of a pairing instability at Λ_c , the flow could be continued to a superconducting state at $\Lambda = 0$. Hence, a divergence of the vertex in the pairing channel at Λ_c is a reliable indicator for a superconducting state. Previously, the leading instability was often determined at a scale $\Lambda_* > \Lambda_c$ at which the vertex exceeds a certain large finite value.¹⁹ This was partially motivated by concerns about the validity of the one-loop truncation in the regime of large effective interactions. However, such a supposedly cautious procedure can lead to incorrect conclusions, since a divergence in the pairing channel is often preceded by a regime of dominant magnetic interactions at scales $\Lambda > \Lambda_c$. On the other hand, we cannot exclude the possibility that the superconducting state obtained from the fRG flow is only metastable. In particular, at and near half-filling there might be an antiferromagnetic ground state that is not signaled by a divergent interaction in the flow, analogously to a first order phase transition which is not signaled by a divergent susceptibility.

A divergence of the magnetic coupling function at a scale Λ below the critical scale for pairing Λ_c would indicate magnetic order coexisting with superconductivity (as the leading instability). We have never encountered such a divergence, in agreement with a previous study

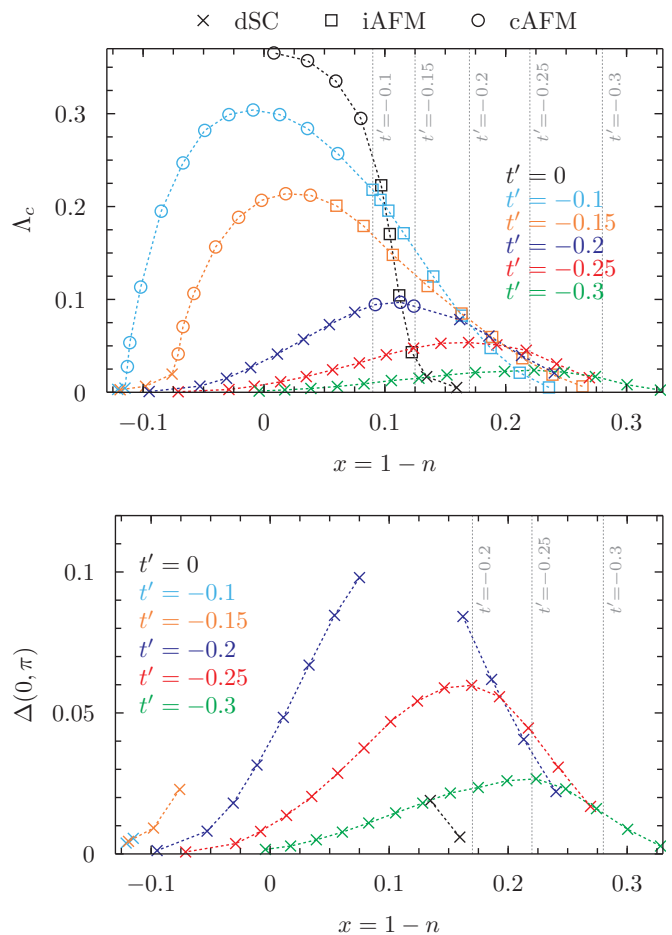


FIG. 2: (Color) Critical scales for the leading instability (top) and d -wave gap amplitude (bottom) as a function of doping for $U = 3$ and various choices of t' . The leading instability is specified by different symbols for Λ_c , and gaps are shown only in the superconducting regime where the flow could be continued to $\Lambda = 0$. The dotted gray vertical lines indicate Van Hove filling for different values of t' .

based on a combination of fRG and mean-field theory, where cases of coexistence with a dominance of pairing turned out to be extremely rare.⁴⁵ Vice versa, a dominant magnetic instability naturally allows for pairing with a smaller energy scale, when the magnetic order does not fully gap the Fermi surface.

A superconducting state at half-filling, as obtained for $t' = -0.2$, is possible only for weak or moderate interactions.^{13,46,47} At strong coupling, the half-filled system is a Mott insulator and magnetic order is the only option for symmetry breaking.

The maximal size of the pairing gap (at “optimal doping”) depends strongly on t' . For $|t'| \leq 0.15$, the leading instability near half-filling is always antiferromagnetic, and d -wave pairing is leading only in a density range away from half-filling where the critical scale and the pairing gaps are already quite small. For $t' = 0$, there

is pairing with a small but visible gap around $x = 0.15$, and, due to the particle-hole symmetry for $t' = 0$, also at $x = -0.15$ (not shown). For $t' = -0.1$ and -0.15 , in the pairing regime at large hole doping, Λ_c and Δ are smaller than the resolution in Fig. 2, and are therefore not plotted. The extended regime of incommensurate antiferromagnetism on the hole doped side is due to Fermi surface nesting. For $|t'| \geq 0.25$, d -wave pairing is the only instability for all densities in the plotted range. The antiferromagnetism found in the hole-doping range around $x = 0.1$ for $t' = -0.2$ is almost degenerate with superconductivity. In this regime, we find commensurate antiferromagnetism due to umklapp scattering between antiferromagnetic hot spots. The largest pairing gap is obtained for $t' = -0.2$ near that antiferromagnetic regime for moderate hole-doping above Van Hove filling. Hence, a substantial but not too large negative value of t' is optimal for obtaining superconductivity with a large gap in the hole-doped system. In the weak and moderate interaction regime, where the one-loop truncation is a controlled approximation, the optimal size of $|t'|$ increases monotonically with U . Hence, we expect an optimal value $t'_{\text{opt}} < -0.2$ for interactions $U > 3$.

IV. CONCLUSION

We have used a fermionic fRG, with a channel decomposition that treats charge, magnetic, and pairing interactions on equal footing, to determine the energy scale and the nature of the leading instabilities in the two-dimensional repulsive Hubbard model at a moderate

interaction strength. Depending on the model parameters, one finds divergent interactions indicating commensurate or incommensurate antiferromagnetism, or d -wave superconductivity, as in previous fRG studies.¹⁹ A recent extension of the fRG for superfluid states allowed us to compute the pairing gap in the superconducting regime. A pairing instability signaled by a divergence in the Cooper channel leads to a superconducting state in all studied cases. We have scanned a wide parameter range, with densities ranging from moderate electron-doping to large hole-doping, and several choices of a next-to-nearest neighbor hopping t' .

The strong t' -dependence resulting from our fRG study is consistent with unbiased QMC simulations of the Hubbard model, where pairing turned out to be too weak to be detected at $t' = 0$,⁴⁸ while evidence for superconductivity was found at $t' = -0.2$.⁴⁹ Band structure calculations by Pavarini et al.⁵⁰ revealed long ago that a substantial hopping amplitude beyond nearest neighbors is beneficial for high-temperature superconductivity in cuprates. Comparing many cuprate compounds, they found empirically that T_c at optimal doping increases systematically with the hopping range.

Acknowledgments

We would like to thank O. K. Andersen, K.-U. Giering, O. Gunnarsson, T. Holder, C. Husemann, B. Obert, M. Salmhofer, H. Yamase, and R. Zeyher for valuable discussions. Support from the DFG research group FOR 723 is also gratefully acknowledged.

-
- ¹ P. W. Anderson, *Science* **235**, 1196 (1987).
² See, for example, D. J. Scalapino, *Phys. Rep.* **250**, 329 (1995).
³ N. E. Bickers, D. J. Scalapino, and S. R. White, *Phys. Rev. Lett.* **62**, 961 (1989).
⁴ A. Neumayr and W. Metzner, *Phys. Rev. B* **67**, 035112 (2003).
⁵ B. Kyung, J.-S. Landry, and A.-M. S. Tremblay, *Phys. Rev. B* **68**, 174502 (2003).
⁶ S. Raghu, S. A. Kivelson, and D. J. Scalapino, *Phys. Rev. B* **81**, 224505 (2010).
⁷ D. Zanchi and H. J. Schulz, *Z. Phys. B* **103**, 339 (1997); *Europhys. Lett.* **44**, 235 (1998); *Phys. Rev. B* **61**, 13609 (2000).
⁸ C. J. Halboth and W. Metzner, *Phys. Rev. B* **61**, 7364 (2000); *Phys. Rev. Lett.* **85**, 5162 (2000).
⁹ C. Honerkamp, M. Salmhofer, N. Furukawa, and T. M. Rice, *Phys. Rev. B* **63**, 035109 (2001).
¹⁰ T. A. Maier, M. Jarrell, T. Pruschke, and M. H. Hettler, *Rev. Mod. Phys.* **77**, 1027 (2005).
¹¹ T. A. Maier, M. Jarrell, T. Pruschke, and J. Keller, *Phys. Rev. Lett.* **85**, 1524 (2000); T. A. Maier, M. Jarrell, T. C. Schulthess, P. R. C. Kent, and J. B. White, *Phys. Rev. Lett.* **95**, 237001 (2005).
¹² E. Khatami, A. Macridin, and M. Jarrell, *Phys. Rev. B* **78**, R060502 (2008).
¹³ E. Gull, O. Parcollet, and A. J. Millis, *Phys. Rev. Lett.* **110**, 216405 (2013).
¹⁴ A. I. Lichtenstein and M. I. Katsnelson, *Phys. Rev. B* **62**, R9283 (2000).
¹⁵ M. Capone and G. Kotliar, *Phys. Rev. B* **74**, 054513 (2006); S. S. Kancharla, B. Kyung, D. Sénéchal, M. Civelli, M. Capone, G. Kotliar, and A.-M. S. Tremblay, *Phys. Rev. B* **77**, 184516 (2008).
¹⁶ M. Aichhorn, E. Arrighoni, M. Potthoff, and W. Hanke, *Phys. Rev. B* **74**, 024508 (2006).
¹⁷ See, for example, H. Yokoyama, M. Ogata, Y. Tanaka, K. Kobayashi, and H. Tsuchiura, *J. Phys. Soc. Jpn.* **82**, 014707 (2013), and references therein.
¹⁸ For reviews of QMC and other numerical results, see E. Dagotto, *Rev. Mod. Phys.* **66**, 763 (1994); N. Bulut, *Adv. Phys.* **51**, 1587 (2002).
¹⁹ For a review of the fRG with a focus on correlated fermion systems, see W. Metzner, M. Salmhofer, C. Honerkamp, V. Meden, and K. Schönhammer, *Rev. Mod. Phys.* **84**, 299 (2012).
²⁰ For general introductions to the fRG, see J. Berges, N. Tetradis, and C. Wetterich, *Phys. Rep.* **363**, 223 (2002);

- P. Kopietz, L. Bartosch, and F. Schütz, *Introduction to the Functional Renormalization Group* (Springer, Berlin, 2010)
- ²¹ T. Baier, E. Bick, and C. Wetterich, Phys. Rev. B **70**, 125111 (2004).
- ²² P. Strack, R. Gersch, and W. Metzner, Phys. Rev. B **78**, 014522 (2008); B. Obert, C. Husemann, and W. Metzner, Phys. Rev. B **88**, 144508 (2013).
- ²³ S. Friederich, H. C. Krahl, and C. Wetterich, Phys. Rev. B **81**, 235108 (2010); Phys. Rev. B **83**, 155125 (2011).
- ²⁴ A. A. Katanin, Phys. Rev. B **70**, 115109 (2004).
- ²⁵ M. Salmhofer, C. Honerkamp, W. Metzner, and O. Lauscher, Prog. Theor. Phys. **112**, 943 (2004).
- ²⁶ R. Gersch, C. Honerkamp, and W. Metzner, New J. Phys. **10**, 045003 (2008).
- ²⁷ A. Eberlein and W. Metzner, Prog. Theor. Phys. **124**, 471 (2010).
- ²⁸ A. Eberlein and W. Metzner, Phys. Rev. B **87**, 174523 (2013).
- ²⁹ C. Karrasch, R. Hedden, R. Peters, T. Pruschke, K. Schönhammer, and V. Meden, J. Phys. Condens. Matter **20**, 345205 (2008).
- ³⁰ C. Husemann and M. Salmhofer, Phys. Rev. B **79**, 195125 (2009).
- ³¹ See, for example, *The Hubbard Model*, edited by A. Montorsi (World Scientific, Singapore, 1992).
- ³² J. W. Negele and H. Orland, *Quantum Many-Particle Systems* (Addison-Wesley, Reading, 1987).
- ³³ C. Wetterich, Phys. Lett. B **301**, 90 (1993).
- ³⁴ The general ansatz for the effective action and the ensuing flow equations are described in detail in Ref. 28.
- ³⁵ In the normal metallic regime above Λ_c this was checked in Ref. 30.
- ³⁶ A. Eberlein, Ph.D. thesis, University Stuttgart, 2013.
- ³⁷ K.-U. Giering and M. Salmhofer, Phys. Rev. B **86**, 245122 (2012).
- ³⁸ H. Yamase and H. Kohno, J. Phys. Soc. Jpn. **69**, 332 (2000); **69**, 2151 (2000).
- ³⁹ E. Fradkin, S. A. Kivelson, M. J. Lawler, J. P. Eisenstein, and A. P. Mackenzie, Annu. Rev. Condens. Matter Phys. **1**, 153 (2010).
- ⁴⁰ T. Holder and W. Metzner, Phys. Rev. B **85**, 165130 (2012).
- ⁴¹ M. A. Metlitski and S. Sachdev, Phys. Rev. B **82**, 075128 (2010); New J. Phys. **12**, 105007 (2010).
- ⁴² C. Husemann and W. Metzner, Phys. Rev. B **86**, 085113 (2012).
- ⁴³ Hot spots are intersections of the Fermi surface with the antiferromagnetic Brillouin zone boundary.
- ⁴⁴ The ratio between gap and Λ_c depends to some extent on the form of the regulator function R^Λ . For the regulator chosen here, one obtains $\Delta/\Lambda_c = 1$ in a reduced BCS model with s -wave pairing.²⁸ For a sharp frequency cutoff one would expect smaller values of Λ_c .
- ⁴⁵ J. Reiss, D. Rohe, and W. Metzner, Phys. Rev. B **75**, 075110 (2007).
- ⁴⁶ S. R. Hassan, B. Davoudi, B. Kyung, and A.-M. S. Tremblay, Phys. Rev. B **77**, 094501 (2008).
- ⁴⁷ M. Sentef, P. Werner, E. Gull, and A. P. Kampf, Phys. Rev. Lett. **107**, 126401 (2011).
- ⁴⁸ T. Aimi and M. Imada, J. Phys. Soc. Jpn. **76**, 113708 (2007).
- ⁴⁹ T. Yanagisawa, J. Phys. Soc. Jpn., **79**, 063708 (2010); New J. Phys. **15**, 033012 (2013).
- ⁵⁰ E. Pavarini, I. Dasgupta, T. Saha-Dasgupta, O. Jepsen, and O. K. Andersen, Phys. Rev. Lett. **87**, 047003 (2001).